Instituto Nacional de Investigación y Tecnología Agraria y Alimentaria (INIA)
Disponible on line en www.inia.es/srf

Investigación Agraria: Sistemas y Recursos Forestales 2009 18(3), 296-313
ISSN: 1131-7965

Combining spectral mixture analysis and object-based classification for fire severity mapping

Ó. Fernández-Manso[1*], C. Quintano[2] and A. Fernández-Manso[3]

[1] Junta de Castilla y León. Agencia de Protección Civil y Consumo. C/ García Morato, 24. 47007 Valladolid (Spain).
[2] Universidad de Valladolid. Departamento de Ingeniería Electrónica. 47014 Valladolid. Spain.
[3] Universidad de León. Departamento de Ingeniería Agraria. Campus de Ponferrada. 24400 Ponferrada, León. Spain.

Abstract

This study shows an accurate and fast methodology in order to evaluate fire severity classes of large forest fires. A single Landsat Enhanced Thematic Mapper multispectral image was utilized with the aim of mapping fire severity classes (high, moderate and low) using a combined-approach based in a spectral mixing model and object-based image analysis. A large wildfire in the Northwest of Spain was used to test the model. Fraction images obtained by Landsat unmixing were used as input data in the object-based image analysis. A multilevel segmentation and a classification were carried out by using membership functions. This method was compared with other simpler in order to evaluate the suitability to distinguish between the three fire severity classes above mentioned. McNemar's test was used to evaluate the statistical significance of the difference between approaches tested in this study. The combined approach achieved the highest accuracy reaching 97.32% and kappa index of agreement of 95.96% and improving accuracy of individual classes.

Key words: wildfire, SMA, OBIA, Landsat ETM+.

Resumen

Cartografía de severidad de incendios forestales a partir de la combinación del modelo de mezclas espectrales y la clasificación basada en objetos

Este estudio presenta una metodología rápida y precisa para la evaluación de los niveles de severidad que afectan a grandes incendios forestales. El trabajo combina un modelo de mezclas espectrales y un análisis de imágenes basado en objetos con el objetivo de cartografiar distintos niveles de severidad (alto, moderado y bajo) empleando una imagen multiespectral Landsat Enhanced Thematic Mapper. Este modelo fue testado en un gran incendio forestal ocurrido en el noroeste de España. Las imágenes fracción obtenidas tras aplicar el modelo de mezclas a la imagen Landsat fueron utilizadas como datos de entrada en el análisis basado en objetos. En este se llevó a cabo una segmentación multinivel y una posterior clasificación usando funciones de pertenencia. Esta metodología fue comparada con otras más simples con el fin de evaluar su conveniencia a la hora de distinguir entre los tres niveles de severidad anteriormente mencionados. El test de McNemar fue empleado para evaluar la significancia estadística de la diferencia entre los métodos testados en el estudio. El método combinado alcanzó la más alta precisión con un 97,32% y un índice Kappa del 95,96%, además de mejorar la precisión de los niveles individualmente.

Palabras clave: incendios forestales, SMA, OBIA, Landsat ETM+

Introduction

Large forest fires are becoming more frequent in Mediterranean areas due to climatic factors and changes in lifestyles and economic conditions. They are one of the most important causes of environmental alteration and land degradation in the Mediterranean Basin, because of the post-fire exposure of bare soil to rainfall (Leone and Lovreglio, 2005). The main consequences of fire on vegetation depend largely on fire severity. In

* Corresponding author: out-fermanos@jcyl.es
Received: 21-11-08. Accepted: 29-10-09.

this study, the term fire severity is defined as the conditions resulting from fire, which can be described by the degree of mortality in above ground vegetation (Ryan and Noste, 1985; Patterson and Yool, 1998; Morgan *et al*., 2001; Rogan and Franklin, 2001; Key and Benson, 2002; Miller and Yool, 2002; Van Wagtendonk *et al*., 2004; Doerr *et al*., 2006). Fire severity maps may complement ecosystem management, providing foresters with baseline data on fire severity and extent required for fire management. Data from these maps may be used to identify areas that have experienced differing fire severity, to plan and monitor restoration and recovery activities, to provide a method for updating current vegetation maps and information for future pre-fire planning (Patterson and Yool, 1998; Brewer *et al*., 2005). It is important therefore, to dispose of techniques to efficiently evaluate fire effects in burned areas.

Considering the extremely broad spatial expansion and often limited access to areas affected by fires, satellite remote sensing provides an important means of gathering information about a burned area in a timely and consistent manner (Rogan and Yool, 2001). Optical satellite imagery from Landsat Enhanced Thematic Mapper (ETM+) has been chosen for this work because the mid-infrared reflectance of vegetation is strongly related to important vegetation canopy characteristics relative to fire effects. It was decided to employ only one post-fire image as it is considered of great interest to find quick and affordable methodology for obtaining fire severity maps avoiding the use of pre-fire images. In doing this, money and time would be saved in terms of obtaining, correcting and normalising images. Landsat missions such as Multi Spectral Scanner (MSS), Thematic Mapper (TM) and ETM+ have been widely used for mapping fire severity (Ryan and Noste, 1985; Milne, 1986; Chuvieco and Congalton, 1988; White *et al*., 1996; Key and Benson, 1999; Key *et al*., 2002; Key and Benson, 2004; Roldán-Zamarrón *et al*., 2006; De Santis and Chuvieco, 2007; González-Alonso *et al*., 2007; Miller and Thode, 2007; Wimberly and Reilly, 2007; Hoy *et al*., 2008; Verbyla *et al*., 2008; Norton *et al*., 2009).

A lack of spectral contrast is partly responsible for the classical errors related to post-fire classifications of burned areas (Koutsias *et al*., 1999): confusion of burned areas with dark land covers (water, dark forests), confusion between slightly burned and sparsely unburned vegetation (problem of the mixed pixels), difficulties in discriminating severity of burning, and confusion between burned vegetation and non-vegetated categories, such as urban areas. To minimize these problems, it has usually been necessary to combine diverse remote sensing systems and a variety of image processing techniques (Justice *et al*., 1993). The range of methods dealing with level-of-damage mapping using post-fire satellite data includes, among others: (1) vegetation indices (White *et al*., 1996; Key and Benson, 1999; Key *et al*., 2002; Díaz-Delgado *et al*., 2003; Chafer *et al*., 2004; Van Wagtendonk *et al*., 2004; Epting *et al*., 2005), (2) linear transformation techniques such as principal components (PC) analysis and Kauth-Thomas transform (KT) (Patterson and Yool, 1998), (3) spectral unmixing (Roldán-Zamarrón *et al*., 2006), etc.

Among the large number of techniques applied for the characterization of burned areas, only a few have quantitatively compared their accuracies (Chuvieco and Congalton, 1988; Koutsias *et al*., 1999), offering little information about the potential and limitations of each technique. To address this issue, this study focuses on a quantitative comparison of four approaches for mapping fire severity using a case of study of a large fire that burned in Northwest Spain, in 1998. We are particularly interested in finding synergies combining both a subpixel-based approach such as Spectral Mixture Analysis (SMA) and an Object-based Analysis Image (OBIA). SMA approach has been widely used due to its ability to cope better with the problem of the mixed pixel and minimize the effects of topography on satellite data (Caetano *et al*., 1994; Caetano, 1995; Caetano *et al*., 1996; Cochrane and Souza, 1998; Rogan and Franklin, 2001; Rogan *et al*., 2002). SMA has the potential of producing results that are directly related to post-fire land management (Caetano *et al*., 1994; Cochrane and Souza, 1998; Roldán-Zamarrón *et al*., 2006). In the case of post-fire assessment, the potential of spectral unmixing relies on the sub-pixel analysis of the materials of a burned area and it has been considered advantageous over vegetation index-based methods, due to its improved capability to distinguish burns from other bare or sparsely vegetated areas (Caetano *et al*., 1996; Díaz-Delgado *et al*., 2001). Despite Object-based classifications are increasingly being used to. In comparison with pixels, image objects carry much more useful information and, therefore, can be characterised by far more properties, such as form, texture, neighbourhood or context, than pure spectral or spectral-derivative information (Baatz and Shäpe, 1999). Object-based classification models have been developed and applied on Landsat TM (Mitri and Gitas, 2002; Mitri and Gitas, 2004a; Mitri and Gitas, 2004b), NOAA-AVHRR images (Gitas *et al*., 2004), and IKONOS images (Mitri and Gitas, 2006; Mitri and Gitas, 2008)

resulting in the accurate mapping of burned areas in the Mediterranean areas.

The main objective of our research is to demonstrate the superior accuracy obtained using a combined approach (SMA plus OBIA) for fire severity mapping with medium-resolution remote sensing image than the obtained by a more traditional approaches.

Materials and methods

Study site description

The study site, 'Tabuyo del Monte', is located in the Sierra del Teleno, in Northern Spain (figure 1). It is a small mountain chain in the South-East (SE) of León province (Spain) with SE aspect, a maximum slope of 11% and elevation ranges from sea level between 850 to 2,100 m.

The climate is Mediterranean with an average annual rainfall between 650 and 900 mm and two or three months of dryness in the summer time. Soil in this area is very sandy and acidic (pH=5.5) (Calvo *et al*., 1998). Currently vegetation is a large natural *Pinus pinaster* Ait. community covering 11,500 ha. Spanish Vegetation Map shows that into the fire scar roughly the 78% was covered by pineland, 18% by shrubs and 4% by Pyrenean oak. Fires have occurred frequently in this community, generally affecting small areas and mostly caused by dry spring-summer storms. However, in September 1998 there was a large fire presumably caused by a military manoeuvre, which burned more than 3,000 ha during four days (between September 13 and 17). This fire is the object of this study.

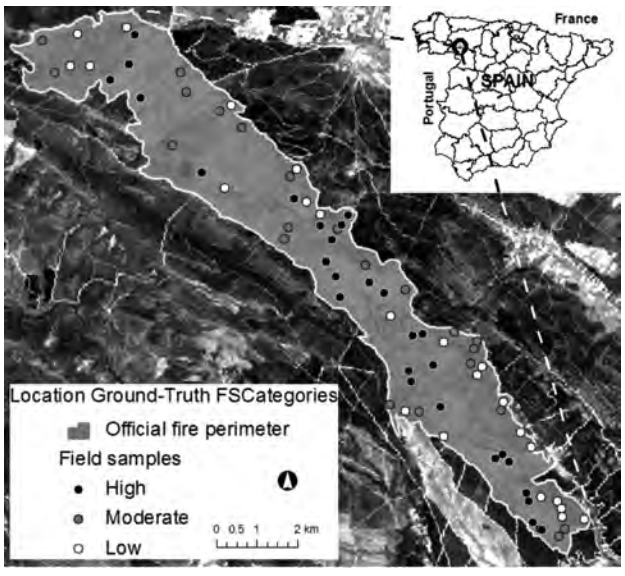

Figure 1. Location of study area in Spain; and location of field samples in the fire scar.

Remotely sensed data

No Landsat cloud-free scenes close to the wildfire date were found so the first scene available corresponded on September, 16 1999. Van Wagtendonk *et al*. (2004) used also one year after the fire occurred post-fire Landsat ETM+ for fire detection. Key (2005) pointed out that extended assessment (EA), (it occurs during the first growing season after fire) may provide more complete representation of actual fire effects. It captures first-order effects that include survivorship and delayed mortality of vegetation present before fire. The former is detected by regrowth from roots and stems of vegetation that burns but remains viable (McCarron and Knapp, 2003; Safford, 2004). Most other first-order effects, such as char, scorch and fuel consumption, are expected to persist until the next growing season, with two exceptions. Areas prone to surface erosion from wind or precipitation may show a decrease in ash cover and an increase of newly exposed mineral soil. Also, canopy foliage that is heat scorched or dies from girdling may drop to ground litter over the interval before EA. Since such effects are more or less complementary in regards to severity assessment, these delayed responses are not expected to significantly alter the remotely sensed magnitude of change detected between initial and extended assessment. In addition, is complete, so the extent of perimeters and distribution of severity represents final conditions.

Preprocessing of remotely sensed images is a preparatory phase that, in principle, improves image quality for further analyses. In this study only a geometric correction was performed. Atmospheric correction was not necessary since only one post-fire image was used to map the fire severity into the fire scar and it was cloud free. In addition, there is a likelihood that uneven implementation of corrections would not necessarily provide a better representation of the mixing space of the SMA model (Elmore *et al*., 2000).

For the geometric correction a set of 22 Ground Control Points (GCP's), selected using the National Topographic Map (Instituto Geográfico Nacional, IGN) at 1:50,000 (UTM 30 T European 1950 mean), and a 25

m-grid size digital elevation model (DEM) were used. A first-order polynomial warp function was applied and a nearest neighbour resampling protocol was then used to preserve original pixel values (Jensen, 1996; Lillesand and Kiefer, 2000). The root mean square error (RMSE) for the transformation was less than 1 pixel. In general, road intersections were used as GCP's since it was possible to locate them in the image. An illumination correction was performed with the C-correction (Teillet *et al*., 1982). This lessens the effects of shadows that may occur due to elevation variations in the landscape.

Field data

In addition to the optical satellite image data, field data were collected in the autumn of 1999 from 72 random plots for fire severity in the Tabuyo burned area (figure 1). Two different datasets were used: one for training and developing the classification rules, and another one for assessing the accuracy of the classification. Separate and independent data were used for training and for accuracy assessment. Despite this time lag, sufficient material remained in the field (scorched leaves on branches and the ground, char on the tree trunks, etc.) for an adequate, qualitative estimate of the degree of severity. Resprouting green leaves did not interfere with these observations.

The field survey plots were sized, with an average area of 0.78 hectare (100 m diameter). Random sampling plots location was correlated with the ETM+ location using a global positioning system. The plots were randoming located within pre-selected large areas with homogenous fire severity levels and low slope gradients by interpreting a 0.7 m-pixel post-fire colour aerial photograph in order to locate in the fire scar representative fire severity categories (scale 1:25,000, digital images orthorectified, mosaicked and examined on-screen in a GIS, captured on October 1998).

Classification of each field plot was determined by visual inspection, based on the observed majority fire severity class within each plot. Three possible fire severity categories were defined according to the degree of scorching vegetation (figure 2). We considered a high-severity, moderate-severity and low-severity as the used by other researchers (e.g., Jakubauskas *et al*., 1990; Turner *et al*., 1994; DeBano *et al*., 1998; Patterson and Yool, 1998; Brown and Smith, 2000; Rogan and Yool, 2001; Arno and Fiedler, 2005). The different fire severity classes were defined as follows:

(1) low: areas where shrubs to 2 m burned and no or partial canopy scorched.
(2) moderate: areas where shrubs incinerated and canopy scorched.
(3) high: areas where shrubs incinerated and canopy completely burned and apparently dead, even though some plants may still be able to sprout.

Data analysis

The development of the main proposed methodology involved two cascaded image analysis techniques: linear spectral mixture (SMA) and object-based image analysis (OBIA).

Image objects were extracted from the fraction images (obtained from SMA algorithm) in the segmentation procedure prior to classification (4th approach). In order to emphasize the benefits achievable using the adopted approach they were provided quantitative evaluations and comparisons with other approaches (1st, 2nd and 3rd) (figure 2).

(1) *First approach: data analysis for Pixel-Based Method (ETM+ISODATA)*

The first approach is a pixel-based image unsupervised classification by Iterative Self-Organizing Data Analysis Technique (ISODATA) (Sunar and Özkan, 2001; Miller and Yool, 2002) to ETM+ image. ISODATA is clustering algorithm that compares the radiometric value of each pixel with predefined number of cluster attractors and shifts the cluster mean values in a way that the majority of the pixels belongs to a cluster. In this case, we interacted with the procedure at the beginning indicating the number of the predefined cluster to be created and the iterations to be carried out and at the end, where it decides which class represents which surface objects and merges or rejects the classes with non-realistic representatives. We masked the satellite image with the official fire perimeter polygon in order to estimate the fire severity categories in the fire scar.

(2) *Second approach: data analysis for Subpixel-Based Method (SMA+ISODATA)*

Because the spatial resolution of Landsat ETM+ imagery is 30 by 30 m, the materials in a given picture element (pixel) are rarely represented by a single physical component. Therefore, in the first stage of this approach (figure 3), a linear spectral model was used which is based on the assumption that the image spectra

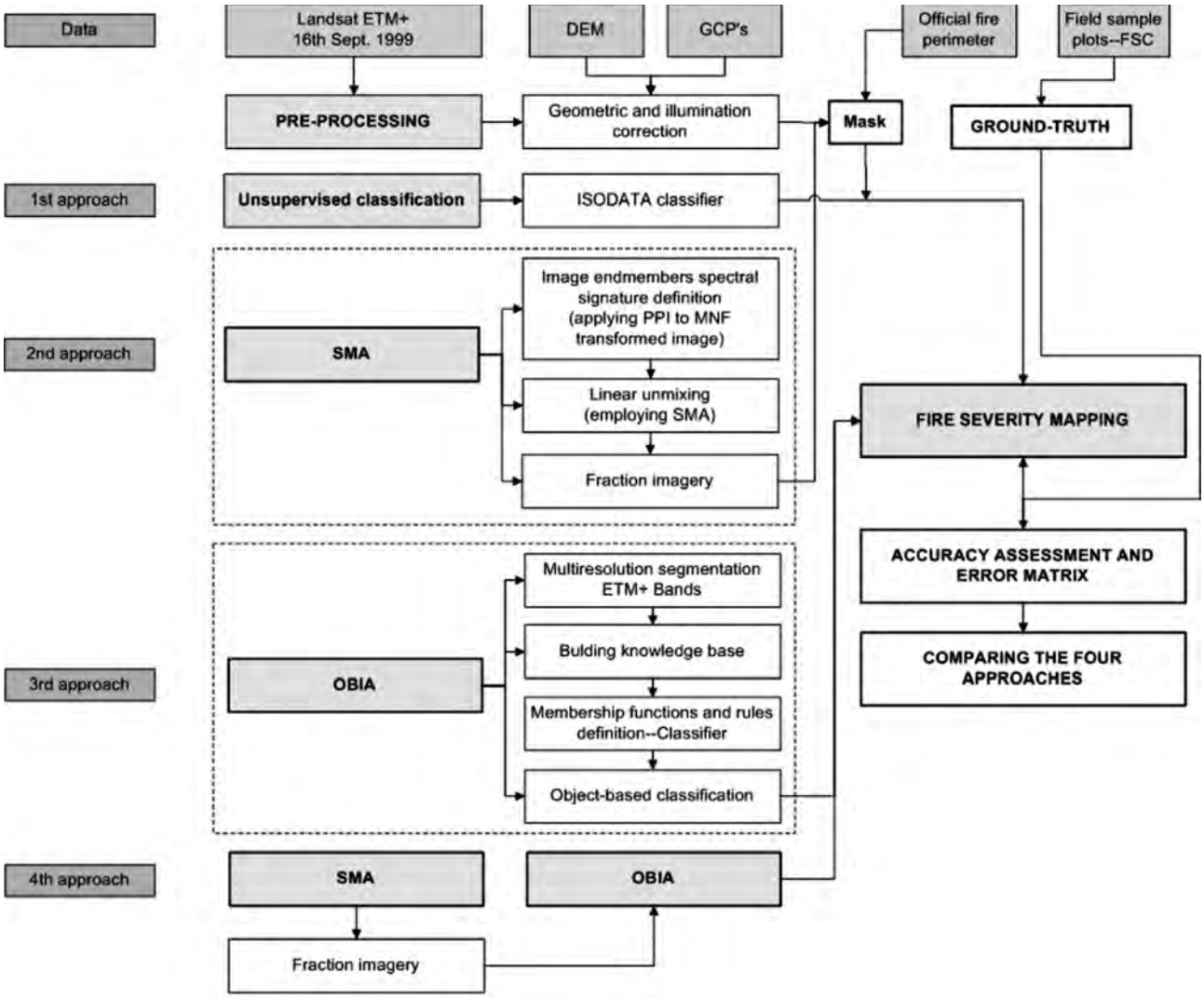

Figure 2. Flowchart of the methodology.

are formed by a linear combination of *n* pure spectra, such that:

$$DN_b = \sum_{i=1}^{n} F_i\ (DN)_{i,b} + \varepsilon_b \qquad [1]$$

where DN_b is the digital number in band *b*, $DN_{i,b}$ is the digital number for endmember *i*, in band *b*, F_i the fraction of endmember *i*, and ε_b is the residual error for each band.

The most common approach is to assume linear unmixing (Shimabukuro *et al*., 1991), although non-linear mixing can occur (Adams *et al*., 1993; Roberts *et al*., 1993). Smith *et al*. (2005) tested the most appropriate mixing model to use (linear or non-linear) in fire severity estimation. Whether the optical mixing was linear or non-linear was largely controlled by the size of the particles present in the ash.

Endmember selection is the most important step in SMA. It determines how accurately the mixture model can represent the spectra. The endmember selection must accommodate the dimensionality of the mixing space. It involves determination of the number of endmembers and the methods to select these endmembers. Possible endmembers, however, are restricted to the number of bands the image data plus one (Hill, 1993; Small, 2004). The Landsat ETM+ sensor has sufficiently low noise that the inherent dimensionality of spectrally diverse images is generally equal to the full six dimensions. We limited this analysis to bands 3, 4, 5, and 7 as White *et al*. (1996) did when they tried to map

fire severity. The definition of appropriate spectral endmembers may be either done using reference endmember from spectral libraries or from the image itself (image endmember). As appropriate reference endmembers were not available for the study site, an approach to extract pure pixels from the image was applied to retrieve image endmembers. For most SMA applications, image endmembers are utilized because they can be easily obtained and can represent spectra measured at the same scale as the image data (Roberts *et al*., 1998a). A minimum noise fraction (MNF) technique (essentially two cascaded principal components transformations) was used to determine the inherent dimensionality of image data, to segregate noise in the data, and to reduce the computational requirements for subsequent processing (Boardman and Kruse, 1994). The data space could be divided into two parts: one part associated with large eigenvalues and coherent eigenimages, and a complementary part with near-unity eigenvalues and noise-dominated images. By using only the coherent portions, the noise was separated from the data, thus improving spectral processing results (ENVI, 2000). It was possible to run an inverse MNF transform using a spectral subset to include only the good bands, or smoothing the noisy bands before the inverse. Separating purer from more mixed pixels reduced the number of pixels to be analyzed for endmember determination and made separation and identification of endmembers easier.

Four new MNF transformed bands were then analysed to find the most spectrally pure (extreme) pixels in the image using a pixel purity index (PPI) classifier. The PPI image was the result of several thousand iterations of the PPI algorithm. The higher values indicated pixels that were nearer to the corners of the n-dimensional data cloud, and were thus relatively purer than pixels with lower values. After the purer pixels were identified in the n-dimensional scatter plot, an inverse-MNF transform was applied to obtain the endmembers spectra, and their spectral response was visually verified using local knowledge (Goodwin *et al*., 2005).

Usually shade could be included either implicitly (fractions sum to 1 or less) or explicitly as an endmember (fractions sum to 1). In our case it was included implicitly (the following equation, $\Sigma Fi = 1.0$, was not included into the equation system of the unmixing model; unconstrained solution).

The least-squares solution is the method most often used for solving the linear mixture model (Smith *et al*., 1990; Shimabukuro and Smith, 1991; García-Haro *et al*., 1996) due to its simplicity and ease of implementation. As the results from the unconstrained solution do not reflect the true abundance fractions of endmembers then the root-mean-square error (RMSE) was used to assess the fit of the model (Adams *et al*., 1993; Roberts *et al*., 1998a) and it is shown in equation (2), where *m* is the number of bands.

$$RMSE = \sqrt{\left(\sum_{b=1}^{m} \varepsilon_b^2\right)/m} \qquad [2]$$

The ISODATA classifier was used to classify fraction image into fire severity categories: high, moderate and low (Sunar and Özkan, 2001; Miller and Yool, 2002; Roldán-Zamarrón *et al*., 2006). Fraction image was masked by fire perimeter polygon before performing unsupervised classification.

(3) *Third approach: data analysis for Object-Based Method (ETM+OBIA)*

Object-based Image Analysis (OBIA) involved two steps: segmentation and classification.

(a) *Image segmentation*

Segmentation is a prerequisite to object-based classification which is the subdivision of an image into separated regions or objects by gathering together many pixels in

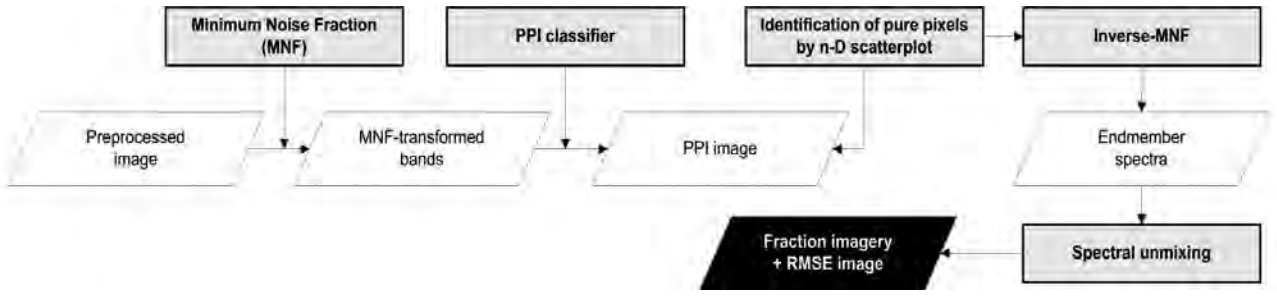

Figure 3. Spectral mixture analysis model.

certain way. In comparison to pixels, image objects carry much more useful information and, therefore, can be characterized by far more properties (such as form, texture, neighbourhood or context) than pure spectral or spectral-derivative information (Baatz and Schäpe, 1999).

The segmentation used in this study was a bottom up region-merging process, starting with one-pixel objects. Throughout the segmentation procedure, the whole image was segmented and image objects were generated based upon several criteria of homogeneity in colour and shape (compactness and smoothness). In a subsequent step smaller image objects (Level 1 or fine scale to define fire severity categories in the fire scar) were merged into bigger ones (Level 2 or coarse scale to define the object boundaries of fire scar). The scale parameter was set to 5 and 20 at level 1 and 2, respectively. The composition of homogeneity criterion was set as follows: colour 0.8 and shape 0.2. For the shape criterion, smoothness was 0.1 and compactness was 0.9.

This process is called multiresolution segmentation, which was used to construct a hierarchical network of image object that simultaneously represented image information in different spatial resolutions (level 1 and 2).

(b) *Object-based classification*

The classification of the image objects was performed by using membership functions based on fuzzy theory combined with user-defined rules. A membership function ranges from 0 to 1 for each object's feature values with regard to the object's assigned class (Navulur, 2007). Spectral, shape, and statistical characteristics as well as relationships between linked levels of the image objects can be used in the rule base to combine objects into meaningful classes (Benz *et al*., 2004). The fuzzy sets were defined by membership functions that identify those values of a feature that are regarded as typical, less typical, or not typical of a class.

(4) *Fourth approach: data analysis for Combined-Based Method (SMA+OBIA)*

After developing fraction images, several methods are commonly used classifying fraction images into different land-cover types, fire severity classes, burned areas, etc. Decision-tree classifiers (DTC) are widely used (e.g., Roberts *et al*., 1998b; Rogan and Franklin, 2001; Rogan *et al*., 2002; Souza *et al*., 2003), as are unsupervised grouping algorithm (ISOSEG) (Quintano *et al*., 2005), and supervised Maximum Likelihood (ML) (Rogan *et al*., 2002; Lu and Weng, 2004).

In our combined approach, an object-based image classification was performed using fraction images obtained in the second approach of this study as input of the model.

Burned vegetation fraction image performed better result in order to fit the image objects on both first and second segmentation levels. The scale parameter was set to 1 and 5 at level 1 and 2, respectively. The composition of homogeneity criterion was set as follows: colour 0.9 and shape 0.1. For the shape criterion, smoothness was 0.2 and compactness was 0.8. As it was done at the third approach, a fuzzy set was defined by membership functions that identified those values of a feature that were regarded as typical, less typical, or not typical of a class.

Classification accuracy was evaluated using ground referenced data. To ensure independence, no training data were used for the validation. Ground referenced data in this context means having been derived from a presumably more accurate data source than the thematic map, in this case from ground visits. The same set of ground data was used in the assessment of the accuracy of the thematic maps obtained by different classifiers in order to compare their suitability in fire severity mapping.

The accuracy assessment was based on confusion matrices, Overall Accuracy (OA), Producer's Accuracy (PA), User's Accuracy (UA) and Kappa Index of Agreement (KIA) statistic (Congalton, 1991). Error matrices were formed with data from thematic map and ground data (Congalton and Green, 1999). McNemar's test was selected to determine significant differences among classifications. Foody (2004) stated that for dependent samples, the statistical significance of the difference between two proportions might be evaluated using McNemar's test. It is a non-parametric test that is based upon confusion matrixes that are 2 by 2 in dimension. The attention is focused on the binary distinction between correct and incorrect class allocations. The McNemar test is based on the standardized normal test statistic (3)

$$Z = \frac{f_{12} - f_{21}}{\sqrt{f_{12} + f_{12}}} \qquad [3]$$

in which f_{ij} indicates the frequency of ground data lying in confusion matrix element i, j. f_{12} and f_{21} are the number of pixels that with one method were correctly classified, while with the other one were incorrectly classified.

Results

General results by approach

The different image processing methods employed and the classification techniques applied with either ISODATA or OBIA yielded varied results (figure 4).

When the unsupervised classification (ISODATA) was applied directly over the satellite image (first approach), the best results for mapping fire severity were reached using bands 3-5 and band 7, 5 iterations and forcing to 3 clusters. This approach could be considered as the best cost-effective method since no image processing technique was applied to the digital number data but it carried out the worst results among the tested approaches.

Regarding second approach, it was obtained a finally four endmembers dataset formed by: soil, two kinds of vegetation (veg1 and veg2) and burned vegetation endmember. The final vegetation 1 (veg 1) endmember was extracted from canopy of pine stands (*Pinus pinaster* Ait.), the vegetation 2 (veg 2) was mainly derived from canopy of *Quercus pyrenaica* Willd., while the soil endmember was located on agricultural areas and the burned vegetation endmember was extracted from the fire scar (figure 5).

Figure 4. Final classified images obtained by means of ISODATA (approaches 1 and 2) and Object-based classification (approaches 3 and 4). Colours corresponding to each class are indicated in the legend.

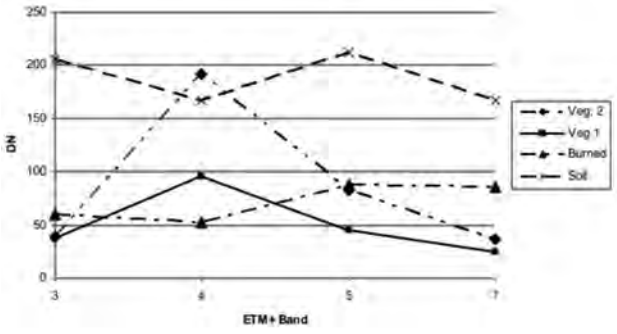

Figure 5. Image endmembers used in the spectral mixing model, expressed in image radiance (DN) for the 3, 4, 5 and 7 reflective ETM+ bands.

Spectral unmixing was performed using the four endmembers derived from the image data leading to 4-fraction images and a root-mean-square error (RMSE) image. The RMSE was calculated for all image pixels. Therefore, the error image was used to assess whether the endmembers were properly selected and whether the number of selected endmembers was sufficient. The value of the RMSE must be lower than the level of noise in the system, in order to guarantee the viability of the results. Landsat ETM+ signal-to-noise value is approximately 2 DN. The unmixing model results were evaluated as proposed by Adams *et al*., 1995. First, we evaluated the RMSE image. Our final model showed low RMSE (<2 DN values). Typically, a reasonable mixing model results in an overall RMS-threshold-error of 2.5 DN values for an image (Roberts *et al*., 1998a). Next, fraction images were evaluated and interpreted in terms of field context and spatial distribution. In this study, final fractions were allowed to be negative or superpositive (Román-Cuesta *et al*., 2005).

Fraction images derived from different combinations of image endmembers were evaluated with visual interpretation and the error extent and distribution in the error fraction image. The criteria used to identify the best suitable fraction images were based on: (1) high-quality fraction images in the fire scar, and (2) relatively low errors in the fire scar. The best results of the spectral mixture analysis for the Tabuyo fire scar are shown in figure 6.

Bright values in these images indicated areas of high fractional abundance for the endmember in question. Bright values on the RMS error image indicated areas that were poorly modelled by the least squares algorithm (values were greater than the 2.5 threshold). A cross-check with the Spanish vegetation map (1:50,000) revealed that these areas with a high RMS error were represented by crops at the time of image acquisition.

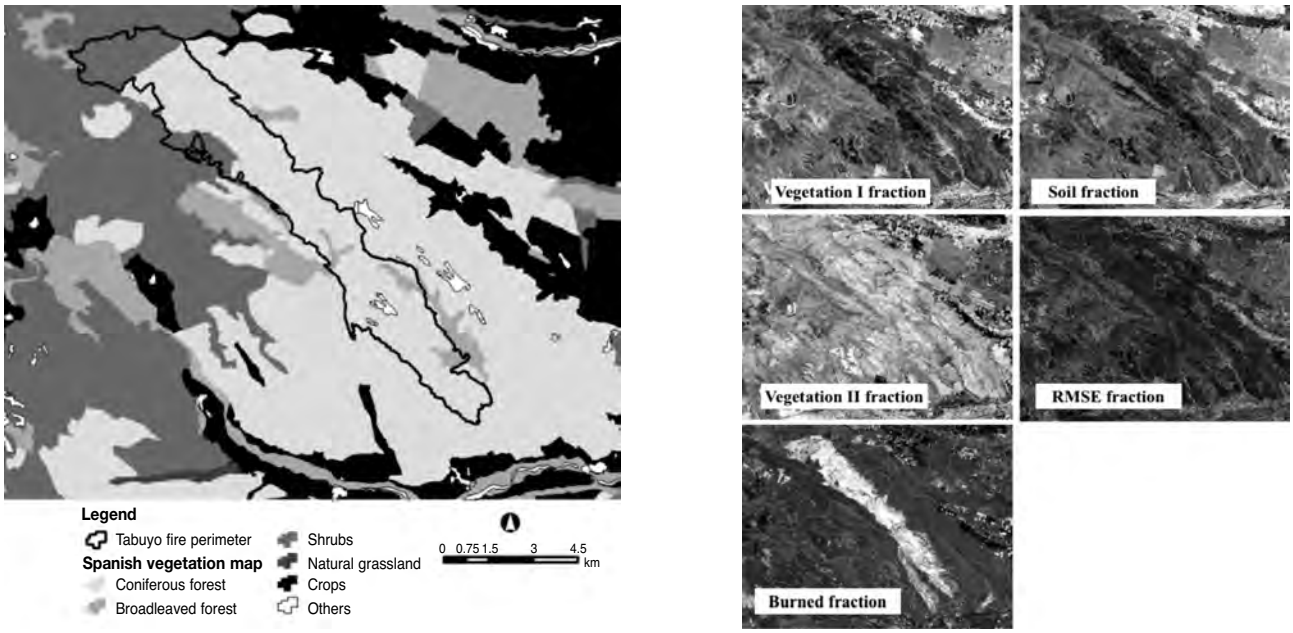

Figure 6. Spanish vegetation map with Tabuyo fire perimeter (left) and spectral unmixing of ETM+ image in fraction imagery (vegetation 1, vegetation 2, burned vegetation, soil and RMSE) (right).

The rest of the image presented a random error distribution. Given the fact that these areas fell outside of the fire scar, we assumed that the endmembers chosen had produced robust and representative image fractions of burned areas, soil and two kinds of vegetation. In this method, fire severity map was carried out by means of applying the ISODATA classifier to burned vegetation fraction image (figure 4).

For the third approach, an object-based analysis was carried out to the ETM+ image. Visual interpretation of different image segmentation results showed that it was extremely beneficial to use band 4 (NIR) and band 7 (SWIR) since they are related with wildfire reflectance values. Official fire perimeter polygon was used as thematic layer in the segmentation in order to a better delineation of fire scar boundaries (figure 7).

Two different levels of image objects representing different scales were created: a fine scale to capture fire severity categories and a coarser scale to define the burned area. Classification at level 2 included the following classes: not burned and possibly burned. This level provided a context to detect the burned area in the image and it was used as super-object information for level 1. Features based on object spectral information (image DN) as well as object contextual information, such as relation to super-objects were used in the classification. The features based on object spectral information were: brightness and ratio B5/ratio B7 to level 2 and the Normalized Burn Ratio (NBR=B4-B7/B4+B7). Existence of super-objects was used as contextual feature. The object NBR was calculated from the NBR values of all *n* pixels forming an image object. Membership functions were adapted for each chosen classification feature. Aerial photos and field notes were used to help interpret the satellite image and select burn thresholds.

For the fourth approach (combined-based approach using SMA and OBIA) two different levels of image objects representing different scales were created also with the aim of capturing fire severity categories. Same class hierarchy as developed in third approach was also adopted (figure 7). Fraction images were used to extract features that were not well distinguishable in the multispectral image. Fuzzy membership functions, which are the knowledge-based part of the classification methodology in eCognition® software, were used to apply fuzzy range to the selected features (which separates a class from other classes, fire severity classes for instance). Because it is necessary to choose the feature to which to apply the membership function, it was explored the feature space to determine which feature(s) best separate the problem classes (fire severity classes). Features based on object information (from fraction image-abundance values) as well as object contextual information, such as neighbourhood and relation to super-objects were used in the classification (figure 8).

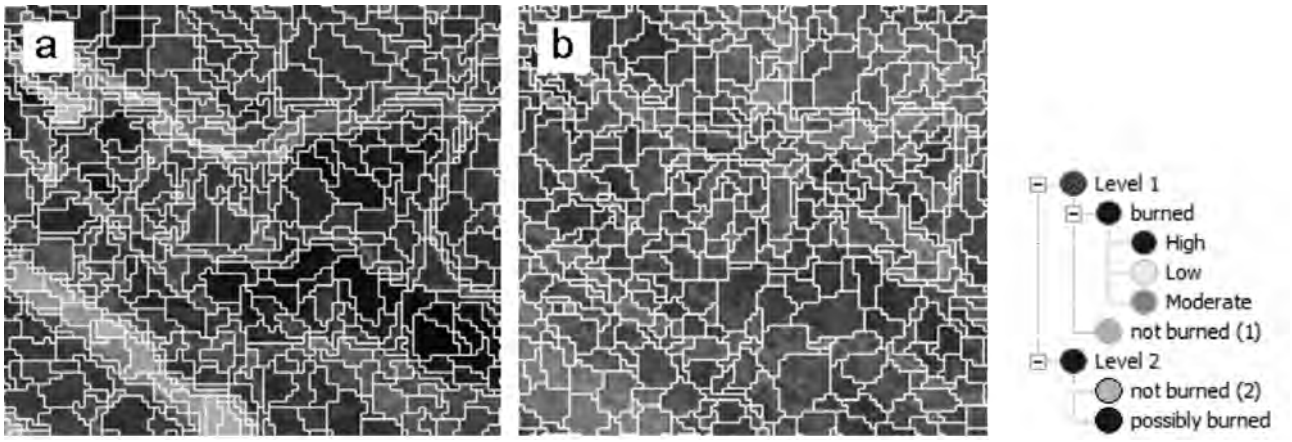

Figure 7. A section of the study area showing the segmentation results on level 1. (a) Approach 3rd. (b) Approach 4th. (c) Class hierarchy created for both approach 3rd and 4th.

The features mean burned vegetation, mean difference to scene burned vegetation and mean soil were useful at differentiating *possibly burned* and not burned from each other in level 2. At level 1, features such as existence of super-objects and mean burned vegetation were the best in separating fire severity classes (low, moderate and high) from each other. Membership functions were adapted for each chosen classification feature by interactively funding the lower and upper limits of the fuzzy ranges on segmentation level 1 for the classes Low, Moderate and High fire severity (figure 9).

Fire severity class areas

The area of fire severity categories varied among the fourth approaches analyzed in this study. Total areas of each approach depend on the combined ability of the classifier and the potential of each technique to separate

Level 2

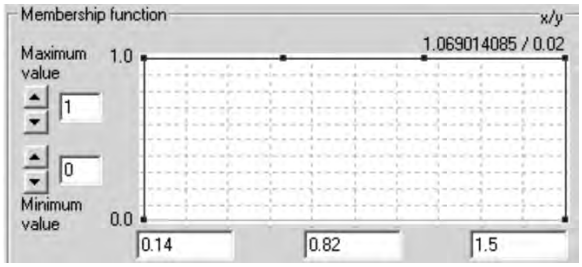

Feature: Mean burned vegetation

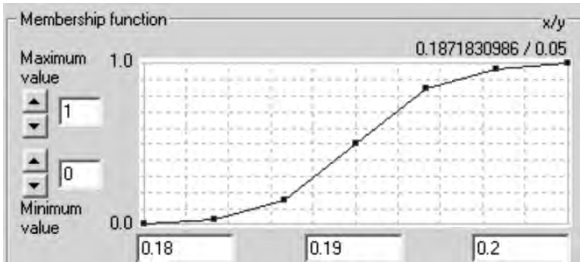

Feature: Mean diff. to scene burned veg.

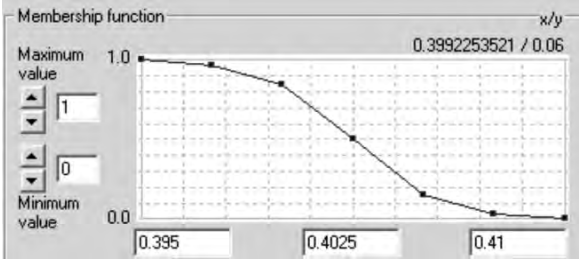

Feature: Mean soil

Figure 8. Membership functions of level 2 and 1 for fourth approach.

Level 1

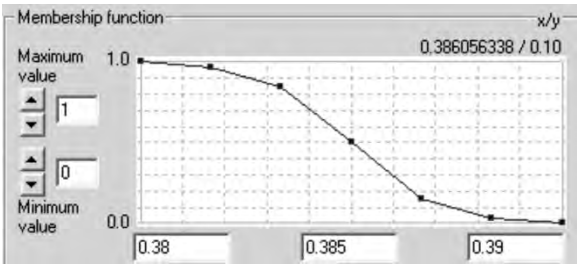

Feature: Mean burned veg for Low

Feature: Mean burned veg for Moderate

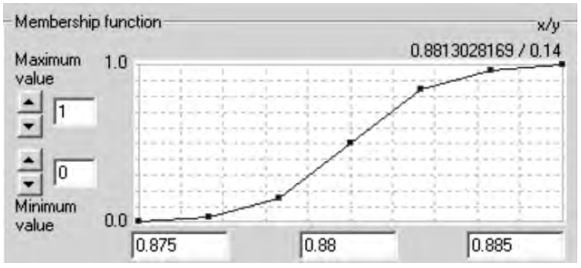

Feature: Mean burned veg for High

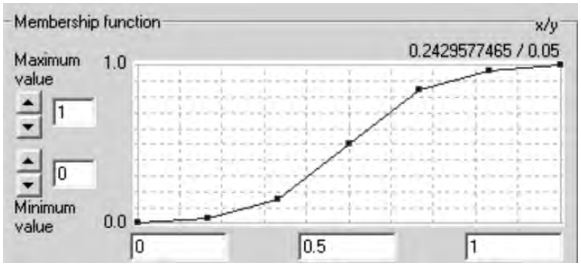

Existence of Possibly burned (L2)

Figure 9. Membership functions of level 1 for fourth approach.

among classes. Total areas of each class and their percentages are shown in table 1.

Accuracy assessments

The classification accuracy between sites visited on the ground and the final fire severity classification displayed different results (table 2). To ensure independence, no training data were used for validation. The remote sensing fire severity values at pixel-level of the plots were then compared to the field survey (100 m-diameter) fire severity classes (table 4).

Regarding the KIA (Kappa Index of Agreement) statistics, the highest values corroborated the overall accuracy (OA) results, with object-based approaches (3 and 4) showing the highest accuracies, in opposite relation with the pixel-based approaches. As happen in overall accuracy, KIA values displayed better values when fraction images were introduced.

A revision of significant differences among KIA statistics based on equation (3) was calculated and showed in table 3. It was apparent that the large differences in accuracy observed between the classifications expressed in terms of proportions of correctly allocated pixels were statistically significant at the 0.1% level of significance. This led to the conclusion that the classification accuracy derived from the four approaches was distinctively different, and the advantage of the approach 4 over the rest of approaches was significant.

An error matrix for each approach was also produced. Based on the User's, Producer's and KIA per class accuracy, individual class accuracies revealed diverse differences among methodologies (table 4).

Table 1. Severity area estimated for each approach

Approach	Methods		High	Moderate	Low	Total area
	Imagery	Classification	(ha)	(ha)	(ha)	(ha)
1	ETM+	ISODATA	686.68	1589.87	1045.15	3309.00
2	Fraction	ISODATA	1097.09	1306.63	917.98	3309.00
3	ETM+	OBIA	1366.65	1358.65	647.21	3309.00
4	Fraction	OBIA	1479.63	1200.87	691.92	3309.00

Table 2. Overall accuracies and KIA statistics for each considered approach

Approach	Methods		Overall accuracy (%)	KIA
	Imagery	Classification		
1	ETM+	ISODATA	59.37	0.3997
2	Fraction	ISODATA	77.67	0.6652
3	ETM+	OBIA	84.67	0.7685
4	Fraction	OBIA	97.32	0.9596

Discussion

Confusion among classes occurred for all approaches even though classes were supposedly quite different in their spectral responses. For the approaches that used ETM+ data instead of fraction imagery as input data for distinguishing among classes, the moderate and low severity classes were confused in the visible and NIR band, but displayed well in the SWIR range. In this regard, White *el al*. (1996) reported Landsat TM band 7 (SWIR) data is useful for distinguishing among different burn severity classes. Regarding approaches using fraction images, they displayed high severity areas characterized by a large amount of burned vegetation and low amount of vegetation and soil, the opposite trend for the low severity areas and an intermediate trend for the moderate severity areas (figure 10). The incorporation of the fraction image into the classification procedure increased the accuracy for both subpixel- and object-based approaches. By employing fraction image the overall accuracy of fire severity classification was improved by 18.30% in subpixel-based and by 12.65% in combined-based approaches (Table 2). Several authors have reported that using fraction images in a classification produces a higher accuracy than results produced by classifying the single sensor bands (Smith *et al*., 1990; Settle and Drake, 1993; Caetano *et al*., 1994; Ustin *et al*., 1996; Huguenin *et al*., 1997; Cochrane and Souza, 1998; Settle and Campbell, 1998; Aguiar *et al*., 1999; Elmore *et al*., 2000; Riaño *et al*., 2002; Theseira *et al*., 2002).

The methods that used ISODATA as classifier performed more moderate and low categories, whereas the OBIA methods (object-based classification), which classified more high and moderate classes. Approach 1 (pixel-based) displayed the highest values for the low severity class, being almost two times larger than the object-based approaches, and lowest values for the high severity class. This was because the ISODATA clustering algorithm only had a one-dimensional space to separate pixels into classes and the means of the classes

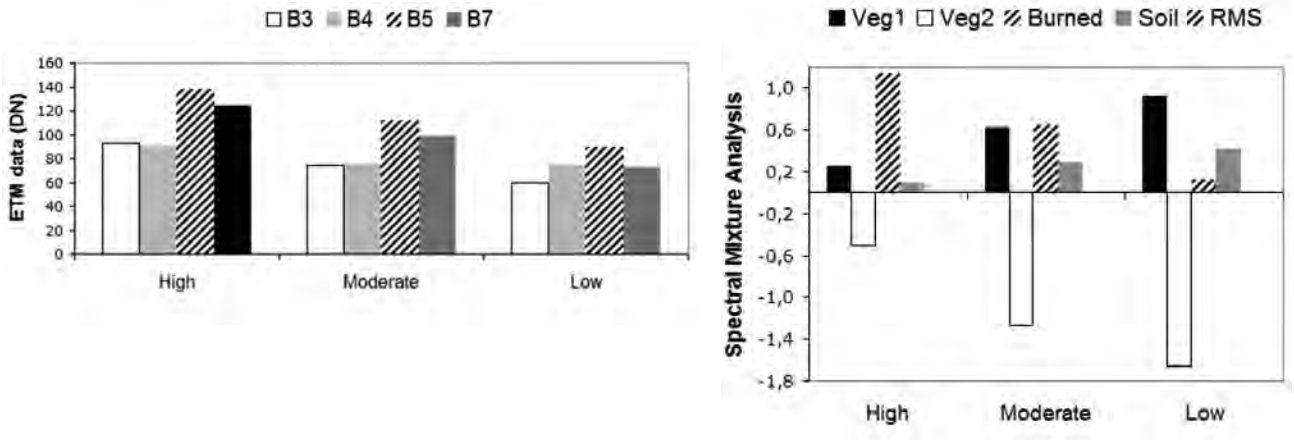

Figure 10. Mean values for each fire severity class (high, moderate and low), for approaches using ETM+ data (left) and for those using fraction imagery (right). Left graphic bars represent the utilized bands: B3, B4, B5 and B7. Right graphic bars represent the different endmembers: vegetation 1, vegetation 2, burned vegetation, soil and error term (RMS). Each sub-section in the right graphic shows the three selected classes: high, moderate and low severity.

Table 3. Significant Zeta statistics (Z=1.96) for all possible pair combinations of the considered approaches (1, 2, 3 and 4)

Approach	1	2	3	4
1		11.09	13.04	15.97
2	S		6.46	11.49
3	S	S		9.22
4	S	S	S	

S= significant. Z=1.96 significant at α=0.05

therefore tended to be uniformly distributed along the one-dimensional space (Miller and Yool, 2002). The better results obtained by approaches that included object-based image analysis into its process are mainly due to the ability of a context-based classification to reduce the speckle in the classification. Obviously, the object-based classification, which first extracts homogeneous regions and then classifies them, avoids the annoying salt-and-pepper effect of the spatially-fine classification results, which is typical of pixel-based analysis. Besides, combined-based approach (SMA/OBIA) performed better results at individual class level. It dealt satisfactory with the problems of classes confusion (burned vegetation and non-vegeted, slighty burned and unburned vegetation) using the information contained into the fraction imagery to the object-based classification and, it had an advantage over the rest of approaches tested by supplying the opportunity to combine contextual and subpixel information (contribution of each surface material in each mixed pixel) into classification which enhanced the accuracy. KIA per class, PA and UA reached high accuracy values, indicating that confusion between problematic classes such as moderate and high were minimized. This implies that introducing fraction image and object-based classification may helpful for improving separability between classes (Table 4).

The proposed method shows potential for further applications such as land cover changes, mining activities, etc. Despite future studies will examine alternative approaches to analyzing images of different resolutions.

Conclusions

Fire severity mapping is an important step by providing operational information for post-fire restoration. This paper investigated the utilization of satellite image and image processing techniques to derive fire severity information. Different approaches were tested in order to obtain accurate fire severity maps. Results showed that fraction images generated by unmixing of a Landsat ETM+ post-fire image can be used as input in an

Table 4. Error matrix and accuracy assessment by fire severity categories for each considered approach

User/Reference Class	High	Moderate	Low	Sum	User/Reference Class	High	Moderate	Low	Sum
Confusion Matrix					**Confusion Matrix**				
High	106	20	1	127	High	203	16	0	219
Moderate	116	94	10	220	Moderate	54	117	8	179
Low	35	91	199	325	Low	0	72	202	274
Sum	257	205	210		Sum	257	205	210	
Producer	0.413	0.459	0.948	**Approach**	Producer	0.789	0.571	0.962	**Approach**
User	0.835	0.427	0.612	**1**	User	0.927	0.654	0.737	**2**
KIA Per Class	0.277	0.191	0.921		KIA Per Class	0.742	0.362	0.941	
User/Reference Class	**High**	**Moderate**	**Low**	**Sum**	**User/Reference Class**	**High**	**Moderate**	**Low**	**Sum**
Confusion Matrix					**Confusion Matrix**				
High	222	44	0	266	High	255	8	0	263
Moderate	35	148	11	194	Moderate	2	197	8	207
Low	0	13	199	212	Low	0	0	202	202
Sum	257	205	210		Sum	257	205	210	
Producer	0.883	0.768	0.909	**Approach**	Producer	0.980	0.897	0.962	**Approach**
User	0.862	0.756	0.950	**3**	User	0.942	0.935	0.971	**4**
KIA Per Class	0.776	0.609	0.921		KIA Per Class	0.989	0.943	0.943	

object-based classification improving the result accuracy. Results complement the findings of a small number of previous studies that support the use of SMA in mapping fire severity due to its ability to produce fractions representative of subpixel components directly related to fire severity. The accuracy of fire severity categories was better combining SMA and OBIA than for the rest of approach tested. McNemar's test was used to evaluate the statistical significance of the difference between the four methods. The difference in accuracy expressed in terms of proportions of correctly allocated pixels was statistically significant at the 0.1% level, which meant that the thematic mapping result using the combined-approach (SMA/OBIA) achieved a much higher accuracy than the rest of approaches.

Acknowledgments

This work was carried out within the framework of the L25-04 project: *Application of new satellite image processing methodologies to estimate forest resources in Castilla y León, Spain*, which is supported by funding of Junta de Castilla y León (Spain).

References

ADAMS, J.B., SMITH, M.O. and GILLISPIE, A.R., 1993. Imaging spectroscopy: interpretations based on spectral mixture analysis. In: Remote Geochemical Analysis: Elemental and Mineralogical Composition (C. M. Pieters and P. A. Englert, Eds.), Cambridge University Press, Cambridge, UK, pp. 145-166.

ADAMS, J.B., SABOL, D.E., KAPOS, V., ALMEIDA, R., ROBERTS, D.A., SMITH, M.O. and GILLESPIE, A.R., 1995. Classification of multispectral images based on fractions of endmembers – Application to Land-Cover change in the Brazilian Amazon. Remote Sensing of Environment, 52 (2), pp. 137-154.

AGUIAR, A.P.D., SHIMABUKURO, Y.E., and MASCARENHAS, N.D.A., 1999. Use of synthetic bands derived from mixing models in the multispectral classification of remote sensing images. International Journal of Remote Sensing, 20 (4), pp. 647-657.

ARNO, S.F., and FIEDLER, C.E., 2005. Mimicking nature's fire: Restoring fireprone forests in the west. Washington, D.C.: Island Press 256 pp.

BAATZ, M. and SCHÄPE, A., 1999. Object-oriented and multi-scale image analysis in semantic networks. In: 2nd International Symposium on Operationalization of Remote Sensing, 16 August 1999 (Enshede: ITC), pp. 16-20.

BENZ, U.C., HOFFMAN, P., WILLHAUCK, G., LINGENFELDER, I. and HEYNEN, M., 2004. Multi-resolution, object-oriented fuzzy analysis of remote sensing data for GIS-ready information. ISPRS Journal of Photogrammetry and Remote Sensing, 58, pp. 239-258.

BOARDMAN, J.W., KNUSE, F.A., and GREEN, R.O., 1995. Mapping target signatures via partial unmixing of AVIRIS data. In: Proceedings of the Fifth JPL Airborne Earth Science Workshop (Pasadena: JPL Publication 95-1), pp. 23-26.

BOARDMAN, J.W. and KRUSE, F.A., 1994. Automated spectral analysis: A geological example using AVIRIS data, north Grapevine Mountains, Nevada. In: Proceedings, ERIM Tenth Thematic Conference on Geologic Remote Sensing, Ann Arbor, MI, pp. 407-418.

BREWER, C.K., WINNE, J.C., REDMOND, R.L., OPITZ, D.W., and MANGRICH, M.V., 2005. Classifying and mapping wildfire severity: A comparison of methods. Photogrammetric Engineering and Remote Sensing, 71, 1311−1320.

BROWN, J.K., and SMITH, J.K., 2000. Wildland fire in ecosystems: Effects of fire on flora. General Technical Report, RMRS-GTR-42-vol. 2. (pp.) Ogden, UT: USDA Forest Service, Rocky Mountain Research Station 257 pp.

CAETANO, M.S., 1995. Burned vegetation mapping in mountainous areas with satellite remote sensing. Master Thesis, University of California, Santa Barbara, pp. 328.

CAETANO, M.S., MERTES, L.A.K. and PEREIRA, J.M.C., 1994. Using spectral mixture analysis for fire severity mapping. In: Proceedings of the 2nd Conference on Forest Fire Research, 11, pp. 667-677.

CAETANO, M.S., MERTES, L.A.K., CADETE, L. and PEREIRA, J.M.C., 1996. Assessment of AVHRR data for characterising burned areas and post-fire vegetation recovery, In: EARSEL Advances on Remote Sensing, 4 (4-XI), pp. 124-134.

CALVO, L., TÁRREGA, R. and LUIS, E., 1998. Space-time distribution patterns of *Erica australis* L. subsp. *arogonensis* (Willk) after experimental burning, cutting, and ploughing. Plant Ecology, 137, pp. 1-12.

CHAFER, C.J., NOONAN, M. and MACNAUGHT, E., 2004. The Post-fire measurement of fire severity and intensity in the Christmas 2001 Sydney wildfires. International Journal of Wild land Fire, 33, pp. 227-240.

CHUVIECO, E. and CONGALTON, R.G., 1988. Using cluster analysis to improve the selection of training statistics in classifying remotely sensed data. Photogrammetric Engineering and Remote Sensing, 54, pp. 1275-1281.

CONGALTON, R., 1991. A review of assessing the accuracy of classifications of remotely sensed data. Remote Sensing of Environment, 37, pp. 35-46.

CONGALTON, R.G. and GREEN, J., 1999. Assessing the accuracy of remotely sensed data: principles and practice. New York, Lewis Publishers, pp. 137.

COCHRANE, M.A. and SOUZA, C.M., 1998. Linear mixture model classification of burned forests in the Eastern Amazon, International Journal of Remote Sensing, 19, pp. 3433-3440.

DEBANO, L.F., NEARY, D. G., and FFOLLIETT, P. F., 1998. Fire's effects on ecosystems. John Wiley & Sons, New York, New York, USA.

DE SANTIS, A. and CHUVIECO, E., 2007. Burn severity estimation from remotely sensed data: Performance of simulation versus empirical models, Remote Sensing of Environment, 108, pp. 422-435.

DÍAZ-DELGADO, R., PONS, X. and LLORET, F., 2001. Fire severity effects on vegetation recovery after fire. The Bigues i Riells wildfire case study. In: 3rd International Workshop on Remote Sensing and GIS applications for Forest Fires Management. New methods and sensors, Chuvieco, E. and Martín, M.P. (Eds.), pp. 152-155. Paris: EARSeL.

DÍAZ-DELGADO, R., LLORET, F. and PONS, X., 2003. Influence of fire severity on plant regeneration by means of remote sensing imagery. *International Journal of Remote Sensing*, 24, pp. 1751-1763.

DOERR, S.H., SHAKESBY, R.A., BLAKE, W.H., CHAFER, C.J., HUMPHREYS, G.S., and WALLBRINK, P.J., 2006. Effects of differing wildfire severities on soil wettability and implications for hydrological response. Journal of Hydrology, 319, 295−311.

ELMORE, A.J., MUSTARD, J.F., MANNING, S.J. and LOBELL, D.B., 2000. Quantifying vegetation change in semiarid environments: Precision and accuracy of Spectral Mixture Analysis and the Normalized Difference Vegetation Index. Remote Sensing of Environment, 73, pp. 86-102.

ENVI, 2000. ENVI User's Guide. Research Systems Inc., Boulder, Colorado, pp. 930.

EPTING, J., VERBYLA, D. and SORBEL, B., 2005. Evaluation of remotely sensed indices for assessing burn severity in interior Alaska using Landsat TM and ETM+. Remote Sensing of Environment, 96, pp. 328-339.

FOODY, G.M., 2004. Thematic map comparison: evaluating the statistical significance of differences in classification accuracy. Photogrammetric Engineering and Remote Sensing, 70, pp. 627–633.

GITAS, I.Z., MITRI, G.H. and VENTURA, G., 2004. Object-based image classification for burned area mapping of Creus Cape, Spain, using NOAA-AVHRR imagery. Remote Sensing of Environment, 92, pp. 409-413.

GONZÁLEZ-ALONSO, F., MERINO-DE-MIGUEL, S., ROLDÁN-ZAMARRÓN, A., GARCÍA-GIGORRO, S. and CUEVAS, J.M., 2007. MERIS Full Resolution data for mapping level-of-damage caused by forest fires: the Valencia de Alcántara event in August 2003. International Journal of Remote Sensing, 28 (3-4), pp. 797-809.

GARCIA-HARO, F.J., GILABERT, M.A. and MELIA, J., 1996. Linear spectral mixture modelling to estimate vegetation amount from optical spectral data. International Journal of Remote Sensing, 17 (17), pp. 3373-3400.

GOODWIN, N., COOPS, N.C. and STONE, C., 2005. Assessing plantation canopy condition from airborne imagery using spectral mixture analysis and fractional abundances. International Journal of Applied Earth Observation and Geoinformation, 7, pp. 11-28.

GREEN, A.A., BERMAN, M., SWITZER, P., and CRAIG, M.D., 1988. A transformation for ordering multispectral data in terms of image quality with implications for noise removal. IEEE Transactions on Geoscience and Remote Sensing, 26, 65-74.

HILL, J., 1993. High precision land cover mapping and inventory with multi-temporal Herat observation data. European Comision, EUR 15271.

HOY, E.E., FRENCH, N.H.F., TURETSKY, M.R., TRIGG, S.N., and KASISCHKE, E.S., 2008. Evaluating the potential of Landsat TM/ETM+ imagery for assessing fire severity in Alaskan black spruce forests. International Journal of Wildland Fire, 17, pp. 500-514.

HUGUENIN, R.L., KARASKA, M.A., BRALICOM, D.V. and JENSEN, J.R., 1997. Subpixel classification of bald cypress and tupelo gum trees in Thematic Mapper imagery. Photogrammetric Engineering and Remote Sensing, 63, pp. 717-725.

JAKUBAUSKAS, M.E., LULLA, K.P. and MAUSEL, P.W., 1990. Assessment of vegetation change in a fire-altered forest landscape. Photogrammetric Engineering and Remote Sensing, 56, pp. 371-377.

JENSEN, J.R., 1996. Introductory digital processing: a remote sensing perspective. Englewood cliffs, New Jersey: Prentice-Hall, pp. 315.

JUSTICE, C.O., MALINGREAU, J.P. and SETZER, A.W., 1993. Satellite remote sensing of fires: potentials and limitations. In: Fire in he Environment: the Ecological, Atmospheric and Climatic Importance of Vegetation Fires, P.J. Crutzen and J.G. Goldammer (Eds), pp. 77-88 (New York: John Wiley and Sons).

KEY, C.H., 2005. Remote sensing sensitivity to fire severity and fire recovery. In: Proceedings of the 5th International

Workshop on Remote Sensing and GIS Applications to Forest Fire Management: Fire Effects Assessment, De la Riva, J., Pérez-Cabello, F. and Chuvieco, E. (Eds): 29-39. Universidad de Zaragoza.

KEY, C.H. and BENSON, N.C., 1999. Measuring and remote sensing of burn severity. In: Proceedings Joint Fire Science Conference and Workshop, vol. II (p. 284), L.F. Neuenschwander, and K.C. Ryan (Eds.). Moscow, ID: University of Idaho and International Association of Wildland Fire.

KEY, C.H, and BENSON, N.C., 2002. Landscape assessment, in fire effects monitoring (FireMon) and inventory protocol: Integration of standardized field data collection techniques and sampling design with remote sensing to assess fire effects. NPS-USGS National Burn Severity Mapping Project.

KEY, C.H., BENSON, N.C., SORBEL, B., ZHU, Z., OHLEN, D., HOWARD, S. and CLEMENT, B., 2002. National Park Service-U.S. Geological Survey National Burn Severity Mapping Project. Retrieved September 30, 2002 from USGS EROS Data Center archive and web site: http://edc2.usgs.gov/fsp/severity/fire_main.asp.

KEY, C.H. and BENSON, N.C., 2004. Ground Measure of Severity, The Composite Burn Index. In: FIREMON: Fire Effects Monitoring and Inventory System, Lutes, R.E. Keane, J.F. Caratti, C.H. Key, N.C. Benson, and L.J. Gangi (Eds.). Gen. Tech Rep. RMRS-GTR-XXX, Ogden, UT: U.S. Department of Agriculture, Forest Service, Rocky Mountain Research Station.

KOUTSIAS, N., KARTERIS, M., FERNÁNDEZ-PALACIOS, A., NAVARRO, C., JURADO, J. NAVARRO, R. and LOBO, A., 1999. Burned land mapping at local scale. In: E. Chuvieco (Ed) Remote Sensing of Large Fires, pp. 157-187, Spring-Verlag, Berlin.

LEONE, V. and LOVREGLIO, R., 2005. Pre and post-fire treatments in Aleppo pine stands: prevention sylviculture and restoration. In: Proceedings II International Conference on prevention strategies of fires in Southern Europe: forest management as a tool for fire prevention. Barcelona, 9-11 may 2005.

LILLESAND, T.M. and KIEFER, R.W., 2000. Remote sensing and image interpretation. 4th ed. New York: Wiley, pp. 724.

LU, D. and WENG, Q., 2004. Spectral mixture analysis of the urban landscape in Indianapolis with Landsat ETM+ imagery. Photogrammetric engineering and remote sensing, 70 (9), pp. 1053-1062.

McCARRON, J.K. and KNAPP, A.K., 2003. C3 shrub expansion in a C4 grassland: positive post-fire responses in resources and shoot growth. American Journal of Botany, 90 (10), pp. 1496-1501.

MILLER, J.D. and THODE, A.E., 2007. Quantifying burn severity in a heterogeneous landscape with a relative version of the delta Normalized Burn Ratio (dNBR). Remote Sensing of Environment, 109 (1), pp. 66-80.

MILLER, J.D. and YOOL, S.R., 2002. Mapping forest post-fire canopy consumption in several overstory types using multi-temporal Landsat TM and ETM data. Remote Sensing of Environment, 82, pp. 481– 496.

MILNE, A.K., 1986. The use of remote sensing in mapping and monitoring vegetational change associated with bush-fire events in eastern Australia. Geocarto International, 1: 25-32.

MITRI, G.H. and GITAS, . ., 2002. The development of an object-oriented classification model for operational burned area mapping on the Mediterranean island of Thasos using LANDSAT TM images. In Forest Fire Research and Wildland Fire safety, Viegas (ed.). Milpress, Rotterdam.

MITRI, G.H. and GITAS, I.Z., 2004a. A performance evaluation of a burned area object-based classification model when applied to topographically and non-topographically corrected TM imagery. International Journal of Remote Sensing, 25, pp. 2863-2870.

MITRI, G.H. and GITAS, I.Z., 2004b. A semi-automated object-oriented model for burned area mapping in the Mediterranean region using Landsat-TM imagery. International Journal of Wildland Fire, 13, pp. 367-376.

MITRI, G.H. and GITAS, I.Z., 2006. Fire type mapping using object-based classification of Ikonos imagery. International Journal of Wildland Fire, 15, pp. 457-462.

MITRI, G.H. and GITAS, I.Z., 2008. Mapping the severity of fire using object-based classification of IKONOS imagery. International Journal of Wildland Fire, 17, pp. 431-442.

MORGAN, P., HARDY, C.C., SWETNAM, T., ROLLINS, M.G. and LONG, L.G., 2001. Mapping fire regimes across time and space: Understanding coarse and fine-scale fire patterns. International Journal of Wildland Fire, 10, pp. 329-342.

NAVULUR, K., 2007. Multispectral image analysis using the object-oriented paradigm. Taylor & Francis group, NW, pp. 165.

NORTON, J., GLENN, N., GERMINO, M., WEBER, K. and SEEFELDT, S., 2009. Relative suitability of indices derived from Landsat ETM+ and SPOT 5 for detecting fire severity in sagebrush steppe. International Journal of Applied Earth Observation and Geoinformation, 11, pp. 360-367.

PATTERSON, M.W. and YOOL S.R., 1998. Mapping fire-induced vegetation mortality using Landsat Thematic Mapper data: a comparison of linear transformation techniques. Remote Sensing of Environment, 65, pp. 132-142.

QUINTANO, C., SHIMABUKURO, Y.E., FERNÁNDEZ, A., and DELGADO, J.A., 2005. A spectral unmixing approach for mapping burned areas in Mediterranean countries. International Journal of Remote Sensing, 26 (7), pp. 1493-1498.

RAMÓN, R.M., RETANA, J., GRACIA, M. and RODRÍGUEZ, R., 2005. A quantitative comparison of methods for classifying burned areas with LISS-III imagery. International Journal of Remote Sensing, 26 (9), pp. 1979-2003.

RIAÑO, D., CHUVIECO, E., USTIN, S., ZOMER, R., DENNISON, P., ROBERTS, D. and SALAS, J., 2002. Assessment of vegetation regeneration after fire through multitemporal analysis of AVIRIS images in the Santo Mountains. Remote Sensing of Environment, 79, pp. 60-71.

ROBERTS, D.A., ADAMS, J.B. and SMITH, M.O., 1993. Discriminating green vegetation, non-photosynthetic vegetation and soils in AVIRIS data. Remote Sensing of Environment, 44, pp. 255-269.

ROBERTS, D.A., BATISTA, G.T., PEREIRA, J.L.G., WALLER, E.K. and NELSON, B.W., 1998a. Change identification using multitemporal spectral mixture analysis: Applications is eastern Amazonia, Remote Sensing Change Detection: Environmental Monitoring Methods and Applications (R. S. Lunetta and C. D. Elvidge, editors). Ann Arbor Press, Ann Arbor, Mich., pp. 137-161.

ROBERTS, D.A., GARDNER, M., and GREEN, R.O., 1998b. Mapping chaparral in the Santa Monica Mountains using multiple endmember spectral mixture models. Remote Sensing of Environment, 65, 267–279.

ROGAN, J. and FRANKLIN, J., 2001. Mapping burn severity in Southern California using spectral mixture analysis. In: Proceedings of the International Geoscience and Remote Sensing Symposium (IGARRS 01), Sydney, Australia, 9-13 July.

ROGAN, J. and YOOL, S.R., 2001. Mapping fire-induced vegetation depletion in the Peloncillo Mountains, Arizona and New Mexico. International Journal of Remote Sensing, 22 (16), pp. 3101-3121.

ROGAN, J., FRANKLIN, J. and ROBERTS, D.A., 2002. A comparison of methods for monitoring multitemporal vegetation change using thematic mapper imagery. Remote Sensing of Environment, 80, pp. 143-156.

ROLDÁN-ZAMARRÓN, A., MERINO-DE-MIGUEL, S., GONZÁLEZ-ALONSO, F., GARCÍA-GIGORRO, S. and CUEVAS, J.M., 2006. Minas de Riotinto (south Spain) forest fire: Burned area assessment and fire severity mapping using Landsat 5-TM, Envisat-MERIS, and Terra-MODIS postfire images. Journal of geophysical research-biogeosciences, 111, G04S11, doi: 10.1029/2005JG000136.

RYAN, K.C., and NOSTE, N.V., 1985. Evaluating prescribed fires. In: USDA (Ed.), Workshop on wildness fires, pp. 230-238.

SAFFORD, H.D., 2004. Fire effects on plant diversity in serpentine vs. sandstone chaparral. Ecology, 85, pp. 539-548.

SETTLE, J. and CAMPBELL, N., 1998. On the errors of two estimators of sub-pixel fractional cove when mixing is linear. IEEE Geoscience and Remote Sensing, 36, pp. 163-170.

SETTLE, J.J. and DRAKE, N.A., 1993. Linear mixing and the estimation of ground cover proportions. International Journal of Remote Sensing, 14, pp. 1159-1177.

SHIMABUKURO, Y.E. and SMITH, J.A., 1991. The least-squares mixing models to generate fraction images derived from remote sensing multispectral data. IEEE Transactions on Geoscience and Remote Sensing, 29, pp. 16-20.

SMALL, C., 2004. The Landsat ETM+ spectral mixing space. Remote Sensing of Environment, 93, pp. 1-17.

SMITH, M.O., USTIN, S.L., ADAMS, J.B. and GILLESPIE, A.R., 1990. Vegetation in deserts: I. A regional measure of abundance from multispectral images. Remote Sensing of Environment, 31, pp. 1-26.

SMITH, A.M.S., WOOSTER M.J., DRAKE, N.A., DIPOTSO, F.M., FALKOWSKI, M.J. and HUDAK, A.T., 2005. Testing the potential of multi-spectral remote sensing for retrospectively estimating fire severity in African savanna environments. Remote Sensing of Environment, 97 (1), pp. 92-115.

SOUZA JR., C., FIRESTONE, L., MOREIRA SILVA, L. and ROBERTS, D., 2003. Mapping forest degradation in the Eastern Amazon from SPOT 4 through spectral mixture models. Remote Sensing of Environment, 87, pp. 494-506.

SUNAR, F., and ÖZKAN, C., 2001. Forest fire analysis with remote sensing data. International Journal of Remote Sensing, 22, 2265−2277.

TEILLET, P.M., GUINDON, B. and GOODENOUGH, D.G., 1982. On the slope-aspect correction of multispectral scanner data. Can. J. Remote Sens. 8, 84-106.

THESEIRA, M.A., THOMAS, G. and SANNIER, C.A.D., 2002. An evaluation of spectral mixture modeling applied to a semi-arid environment. International Journal of Remote Sensing, 23, pp. 687-700.

TURNER, M.G., HARGROVE, W.W., GARDNER, R.H. and ROMME, W.H., 1994. Effects of fire on landscape heterogeneity in Yellowstone National Park, Wyoming. Journal of Vegetation Science, 5, pp. 731-742.

USTIN, S.L., HART, Q.J., DUAN, L. and SCHEER, G., 1996. Vegetation mapping on hardwood rangelands in California. International Journal of Remote Sensing, 17, pp. 3015-3036.

VAN WAGTENDONK, J.W., ROOT, R.R. and KEY, C.H., 2004. Comparison of AVIRIS and Landsat ETM+ detection capabilities for burn severity. Remote Sensing of Environment, 92, pp. 397-408.

VERBYLA, D.L., KASISCHKE, E.S. and HOY, E.E., 2008. Seasonal and topographic effects on estimating fire severity from Landsat TM/ETM+ data. International Journal of Wildland Fire, 17, pp. 527-534.

WHITE, J.D., RYAN, K.C., KEY, C.C. and RUNNINGS, S.W., 1996. Remote sensing of forest fire severity and vegetation recovery. International Journal of Remote Sensing, 6, pp. 125-136.

WIMBERLY, M.C. and REILLY, M.J., 2007. Assessment of fire severity and species diversity in the southern Appalachians using Landsat TM and ETM+ imagery. Remote Sensing of Environment, 108 (2), pp. 189-197.